Materials Advances

ROYAL SOCIETY OF CHEMISTRY

PAPER

View Article Online
View Journal | View Issue

Cite this: *Mater. Adv.*, 2023, 4, 1555

Functionalization of cellulose nanofibrils to develop novel ROS-sensitive biomaterials†

Carlos Palo-Nieto,*[a] Anna Blasi-Romero,[a] Corine Sandström,[b] David Balgoma,[c] Mikael Hedeland,[c] Maria Strømme[a] and Natalia Ferraz *[a]

Wood derived cellulose nanofibrils (CNFs) have emerged as an interesting material for biomedical applications. Functionalization of the nanofibrils with bioactive molecules is a potent tool to tailor CNF materials for specific applications in biomedicine. The present work proposes the functionalization of CNFs with a reactive oxygen species (ROS)-sensitive oligopeptide to develop a novel CNF-based material for the treatment of medical conditions associated with high levels of ROS such as chronic wounds. Oligoproline peptides of two different lengths (5 and 10 proline units) were covalently incorporated onto the CNF surface, several water-based chemical approaches were explored and the reaction conditions to maximize peptide substitution and the degree of fibre crosslinking were optimized. The chemical structure, degree of peptide substitution, degree of fibre crosslinking, surface morphology and ROS-sensitivity of the oligoproline–CNF materials were characterized. Double-crosslinked CNF hydrogels (Ca^{2+}–oligoproline–CNF) were further prepared and the ability of the hydrogels to protect cells from an oxidative environment was investigated *in vitro* with human dermal fibroblasts, as a first evaluation of the potential of the novel CNF material to be used in chronic wound therapies. Optimization of the reaction conditions resulted in a degree of peptide substitution of 102 ± 10 μmol g^{-1} CNF irrespective of the oligoproline length and a degree of crosslinking of 55–80% depending on the number of proline units. The results showed that the oligoproline covalently attached to CNFs *via* carbodiimide chemistry maintained its ability to respond to ROS and that the responsiveness in terms of viscoelastic properties depended on the length of the oligopeptide, with the hydrogel being more responsive when functionalized with 10 proline units compared with 5 proline units. Furthermore, the double crosslinked Ca^{2+}–oligoproline–CNF hydrogels promoted the survival of human dermal fibroblasts exposed to high levels of ROS. This study is the first one to provide an insight into the development of ROS-sensitive materials based on CNFs and opens up possibilities for further investigation on the use of these novel materials in chronic wound care.

Received 25th November 2022,
Accepted 7th February 2023

DOI: 10.1039/d2ma01056a

rsc.li/materials-advances

Introduction

The increasing concern about the sustainability of resources has contributed to the growing interest in wood-derived cellulose nanofibrils (CNFs) for a wide range of applications. CNFs are obtained by the mechanical disintegration of wood fibres, a process that is usually combined with chemical and/or enzymatic pre-treatments of the wood pulp to facilitate the fibrillation and thus reduce the energy consumption in CNF production.[1] CNFs, whose typical dimensions are 3–50 nm in diameter and up to several micrometres in length, combine inherent cellulose properties such as hydrophilicity, mechanical strength and a broad spectrum of possible chemical modifications with nanomaterial characteristics like high specific surface area, high aspect ratio, and tailorable optical, mechanical and rheological properties.[2,3] CNFs form colloidal suspensions in water, with the gel network maintained by the entanglement of the fibres, hydrogen bonds, electrostatic and van der Waals interactions.[4]

CNF gel suspensions can be further processed to obtain films, aerogels and self-standing hydrogels, and their properties are exploited to develop CNF-based materials for a wide range of applications, ranging from food and pharmaceutical packaging, textiles and green electronics to biomedicine.[5] CNF hydrogels are particularly interesting for biomedical applications such as drug delivery, wound healing dressings and tissue engineering scaffolds due to their high water content, porosity and ability to mimic the extracellular matrix.[6,7] Moreover, functionalization of

[a] *Nanotechnology and Functional Materials, Department of Materials Science and Engineering, Uppsala University, Uppsala, Sweden. E-mail: natalia.ferraz@angstrom.uu.se, carlos.nieto@angstrom.uu.se*
[b] *Department of Molecular Sciences, Swedish University of Agricultural Sciences, Uppsala, Sweden*
[c] *Department of Medicinal Chemistry, Analytical Pharmaceutical Chemistry, Uppsala University, Uppsala, Sweden*

† Electronic supplementary information (ESI) available. See DOI: https://doi.org/10.1039/d2ma01056a

the nanofibres gives the opportunity of modifying the physicochemical properties as well as tailoring the interaction with biological systems to address the demands of specific biomedical applications.[8,9] For example, strong and stable gels can be obtained by chemical crosslinking of the nanofibres,[4] while functionalization with bioactive molecules allows surpassing the bioinert characteristic of CNFs and tailoring CNF hydrogels for specific applications.[10,11]

The development of reactive oxygen species (ROS)-sensitive materials for biomedical applications such as gene delivery, biosensing and cell protection has recently gained attention.[12,13] ROS-sensitive moieties have been incorporated in nanoparticles, polymers and hydrogels to aid in the treatment of pathological conditions associated with high levels of ROS such as cancer and inflammatory, cardiovascular and neurodegenerative conditions.[14,15] Polypeptides, due to their biocompatibility and biodegradability, are great candidates for ROS-sensitive moieties. In particular, it has been demonstrated that peptides containing proline residues are especially susceptible to oxidative degradation.[16,17] Moreover, proline-rich peptides are widespread in nature and have shown antimicrobial, immunomodulatory and/or antioxidant properties.[18–20] Polymeric scaffolds containing proline oligomers have been synthesized before as ROS-responsive biomaterials, and their ability to undergo structural changes in oxidative environments and protect cells have been proven.[21–23]

Chronic wounds are characterized by elevated levels of ROS, pro-inflammatory cytokines and degradative proteases, resulting in reduced concentrations of growth factors and proteinase inhibitors and an imbalance in the wound equilibrium.[24,25] While traditional wound care relies on the use of wound dressings that protect the wound from further trauma and promote a moist environment; chronic wound care demands therapies that not only provide an optimal local healing milieu but that also stimulate the healing.[26,27] Cell-based therapy and the delivery of growth factors have been listed as promising strategies to accelerate the healing and promote the resolution of hard-to-heal wounds.[26] However, a harsh chronic wound environment, *i.e.* high levels of ROS and proteases, limits the success of such therapies.[28] Thus, the development of wound dressings able to control the levels of ROS in a chronic wound environment could aid in bringing forward the use of therapies based on cell and growth factor delivery.

We have previously demonstrated the ability of Ca^{2+}-crosslinked CNF hydrogels to support the healing of acute wounds.[29–31] The easily modifiable nature of CNFs can be exploited to further develop a Ca^{2+}-crosslinked hydrogel to address the treatment needs in chronic wound care. In the present work, we propose to functionalize CNFs with the ROS-sensitive linker oligoproline to endow the CNF-based wound dressing with ROS-scavenger properties and foresee a cell protective effect of the novel CNF hydrogel. Herein, we describe the covalent incorporation of oligoproline peptides onto the CNF surface, exploring different water-based chemical approaches and optimizing the reaction conditions to maximize peptide substitution and the degree of fibre crosslinking. The oligoproline–CNF materials are characterized in terms of chemical structure, degree of peptide substitution, degree of fibre crosslinking, surface morphology and ROS-sensitivity. Finally, the ability of the new double-crosslinked CNF hydrogels (Ca^{2+}–oligoproline–CNF) to protect cells from an oxidative environment is investigated *in vitro* with human dermal fibroblasts, as a first evaluation of the potential of the novel CNF material to be used in chronic wound therapies.

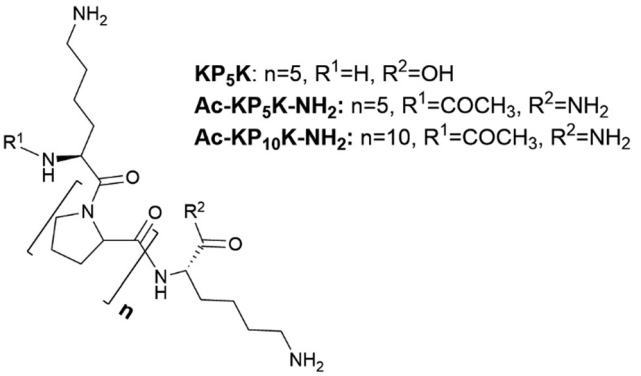

Fig. 1 ROS-sensitive oligoproline peptides used in this work.

Experimental

Materials and methods

Chemicals and reagents. Carboxymethylated-CNF (c-CNF, carboxyl group content of 1800 μmol g^{-1} dry CNF, and degree of substitution of 0.3), provided by RISE Bioeconomy (Stockholm, Sweden), was produced from commercial never-dried bleached sulfite softwood dissolving pulp (lignin content < 1.5%, xylose < 1.7%, mannose < 1.8%, Domsjö Fabriker AB, Örnsköldsvik, Sweden) by sodium chloroacetate-mediated oxidation.[32] *N*-(3-dimethyolaminopropyl)-*N*′-ethylcarbodiimide hydrochloride (EDC), *N*-hydroxysuccinimide (NHS), sodium (meta)periodate ($NaIO_4$), sodium cyanoborohydride ($NaCNBH_3$) and live/dead staining kit were purchased from Sigma-Aldrich Sweden AB, Sweden, and used as received. Oligoproline peptides were purchased from Hangzhou Go Top Peptide Biotech (Hangzhou, China). DMEM-F12 medium, fetal bovine serum (FBS), penicillin and streptomycin were obtained from ThermoFisher Scientific (Waltham, MA, USA).

Oligoproline peptides. Oligoproline peptides with two different lengths, 5 and 10 proline units, were used in this work. The amino acid lysine was incorporated in both ends of the oligoproline (KP_5K) in order to target the reaction with carboxyl groups in c-CNF. These peptides were further modified in order to minimize side reactions and increase the reaction efficiency, *i.e.* α-amine and carboxylic acid of the terminal lysines were *N*-acetylated and amidated, respectively (*N*-α-acetyl-KP_5K amide (Ac-KP_5K-NH_2) and *N*-α-acetyl-$KP_{10}K$ amide (Ac-$KP_{10}K$-NH_2)). Fig. 1 shows the structure of the oligoproline peptides under study.

Covalent incorporation of oligoproline peptides onto cellulose nanofibrils. ROS-sensitive oligoproline peptides were covalently incorporated onto c-CNF using the well-known synthetic routes, amine coupling through EDC/NHS and reductive

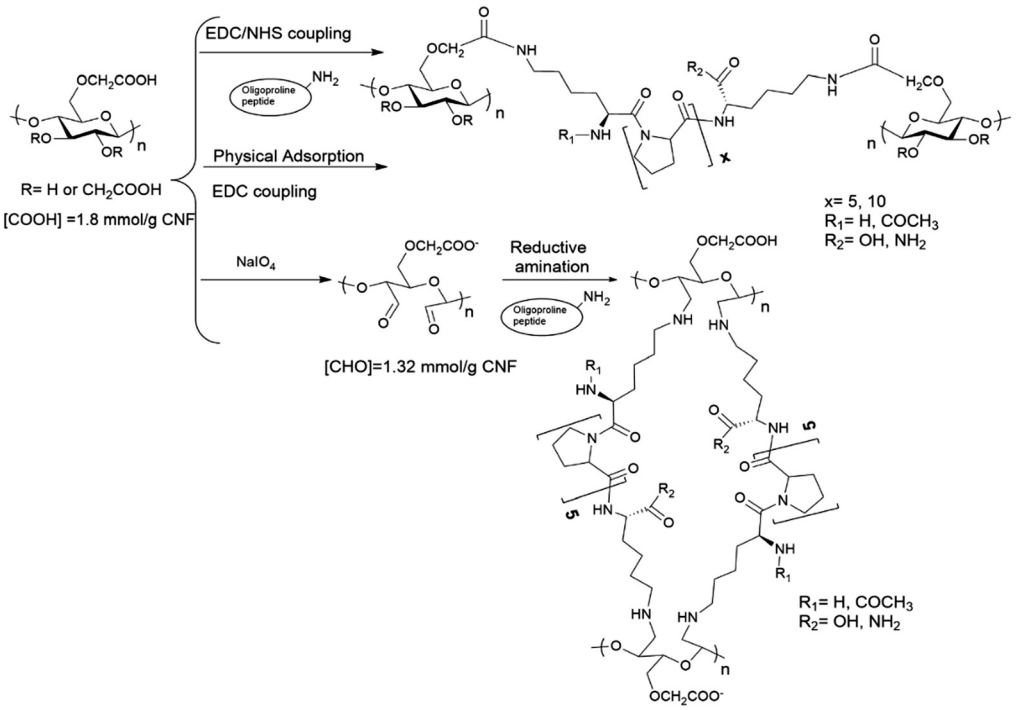

Fig. 2 Synthetic routes used to covalently incorporate oligoproline peptides onto cellulose nanofibrils. Here the intended crosslinking of the fibres is illustrated.

amination (Fig. 2). The aim was to explore different reaction conditions to obtain a controlled covalent immobilization of oligoproline onto the nanofibre surface while promoting the covalent crosslinking of the nanofibres by the peptide. Synthetic routes are briefly described below.

EDC/NHS coupling. A c-CNF suspension (50 g of 2 wt% suspension, 1 g dry c-CNF, 1.8 mmol COOH) was homogenised by stirring in 250 mL of deionized water. Next, a solution containing EDC (674 mg, 3.6 mmol) and NHS (607 mg, 5.4 mmol) was added to the suspension, the pH was adjusted to 5.5–6.0 by adding 0.1 M HCl and left stirring for 30 minutes for activation of the carboxylic acids. Afterwards, the suspension was centrifuged and washed two times with deionized water in order to remove the residual EDC and NHS. Thereafter, a solution containing the peptide (KP_5K, Ac-KP_5K-NH_2 or Ac-$KP_{10}K$-NH_2, 0.18 mmol or 0.9 mmol) was added dropwise to the activated c-CNF. Then, the pH was adjusted to 7.5–8.0 by adding 0.1 M NaOH and the reaction mixture was allowed to proceed overnight under continuous stirring at 25 °C. For purification, the modified material was washed several times with 0.1 M NaOH/0.05 M $NaHCO_3$ buffer (pH = 11) in order to remove the unreacted peptide potentially entrapped within the nanofibres, as well as impurities. The material was washed until the free peptide was no longer detected in the supernatant by liquid chromatography–mass spectrometry (LC-MS, Fig. S1, ESI†).

Physical adsorption followed by covalent immobilization. A reaction mixture containing c-CNF (50 g of 2 wt% suspension, 1 g dry c-CNF, 1.8 mmol COOH) and the peptide Ac-KP_5K-NH_2 (0.18 mmol) was homogenised in 250 ml of deionized water. Then, the mixture was stirred for 1h at pH 5 and 25 °C, in order to favour electrostatic interactions between the c-CNF negative charges and the positively charged peptide. Subsequently, a water solution containing EDC (674 mg, 3.6 mmol) was added to the reaction mixture and stirred for 16 h at 25 °C. Afterwards, the material was washed several times with 0.1 M NaOH/0.05 M $NaHCO_3$ buffer (pH = 11) until the free peptide became no longer detected in the supernatant by LC-MS.

Reductive amination of periodate-oxidized c-CNF. Oxidation at the C2–C3 position of 1.0 g dry c-CNF (50 g of 2 wt% suspension) was carried out using $NaIO_4$ (1.32 g, 1 : 1 $NaIO_4$: anhydroglucose unit) at 25 °C for 8 h under dark conditions, and thereafter the remaining $NaIO_4$ was washed out three times with deionized water. Oxidized c-CNF (1.32 mmol [CHO] per g CNF, determined by the NH_2OH method)[33] was then incubated with the oligoproline peptide (KP_5K or Ac-KP_5K-NH_2, 0.132 mmol or 0.66 mmol) at 25 °C (pH 4.5) for 16h. Afterwards, the material was washed with 0.1 M NaOH/0.05 M $NaHCO_3$ buffer (pH = 11) in order to remove the non-covalently bonded peptide.

Material characterization

Chemical structure. The chemical structure of the oligoproline-CNF materials was characterized by solid state nuclear magnetic resonance (NMR) spectroscopy. The NMR spectra were obtained on a Bruker Avance III 600 MHz spectrometer using a double-resonance 4 mm (^{1}H&^{19}F)/(^{15}N-^{31}P) CP-MAS probe and 4 mm ZrO_2 rotors. The ^{13}C cross-polarization (CP) magic angle spinning (MAS) NMR spectra were recorded at a spinning frequency of 12 KHz, a contact time of 1–2 ms and a repetition delay of 3–5 s. The experiments were performed at 298 K.

Peptide content. The oligoproline peptide content in the functionalized CNF materials was determined by elemental analysis of the total nitrogen content. The technique used for the determination of CHN is based on the quantitative dynamic flash combustion method. Oligoproline-CNF freeze-dried samples were submitted to MEDAC LTD Analytical and chemical consultancy services in Chobham (United Kingdom). There, the Thermo FlashEAR 1112 instrument was used for nitrogen quantification. The weight percentage of nitrogen in oligoproline-CNF was converted to mmol oligoproline per g CNF.[34,35]

Degree of covalent crosslinking. The ninhydrin assay was used to determine the degree of crosslinking of the oligoproline-CNF materials by quantifying unreacted primary amines in peptides covalently attached to c-CNF (*i.e.* peptides anchored to the nanofibrils by only one end). The ninhydrin test described by P. Eiselt *et al.*[36] was slightly modified. Briefly, 250 μL of 10 mg ml^{-1} oligoproline-CNF suspension was mixed with 750 μL of 1 M acetate buffer (pH 5), and 1 mL of 2% (w/v) ninhydrin solution was added. The mixture was kept in a closed vial to avoid evaporation and immersed in a hot water bath at 75 °C for 15 min. Then, 15 mL of ethanol : water (1 : 1, v/v) was added. The reaction mixture was cooled down at room temperature for 1 h in the dark. Absorbance at 570 nm was measured using a spectrophotometer (UV-1800, Shimadzu, Kyoto, Japan). The concentration of amino groups was calculated using a calibration curve prepared with the AcP_5K peptide (oligoproline peptide presenting only one reactive side, *i.e.* one of the terminal lysine is acetylated). CNF suspension without incorporated peptide was used as turbidity interreference control. AcP_5K-CNF, *i.e.* CNF functionalized with the oligoproline peptide presenting only one reactive side, was assayed as a non-crosslinking control (0% degree of crosslinking).

Considering that the free amino group detection in the oligoproline-CNF material is from peptides anchored to the nanofibres by only one end, the degree of crosslinking was calculated by the difference between the total peptide content and the free amino group content according to eqn (1):

$$\text{Degree of crosslinking}(\%) = \frac{\text{total peptide content}^1 - \text{free amino group content}^2}{\text{total peptide content}^1} \times 100 \quad (1)$$

Here [1] is obtained from the elemental analysis; and [2] from the ninhydrin assay.

Oligoproline-CNF response to ROS

To investigate the response to ROS of the covalently attached oligoproline, the KP_5K-CNF material (110 μmol peptide per g CNF) was suspended in phosphate-buffered saline (PBS, pH 7.4), followed by the addition of H_2O_2 and $CuSO_4$ (10 equivalents and 0.05 equivalents with respect to the peptide content, respectively).[22] The reaction mixture was incubated in the dark at 37 °C for 4 days (fresh $H_2O_2/CuSO_4$ was added daily) and aliquots were taken every 24 h and frozen at −20 °C, stopping the oxidation reaction before liquid chromatography-mass spectrometry (LC-MS) analysis. The KP_5K oligopeptide incubated in the absence of $H_2O_2/CuSO_4$ and c-CNF tested in both oxidative and non-oxidative conditions served as controls, while the oxidative degradation of the KP_5K oligopeptide served as reference.

The peptides and the products of oxidation were separated by LC-MS on an Acquity UPLC coupled to a Synapt G2S Q-ToF mass spectrometer. The separation column was an Acquity BEH C18 2.1 × 150 mm (1.7 μm of particle size), the column temperature was 25 °C, and the flow-rate was 0.175 mL min^{-1}. The separation was achieved by a gradient of mobile phases A (water : methanol 95 : 5 5 mM NH_4HCO_2) and B (methanol 5 mM NH_4HCO_2). The elution started at 100% A and was maintained until minute 2. From minute 2 to minute 12, separation was achieved by a non-linear gradient (Waters' concave curve 9, *i.e.* %B = 100 × $[(t - 2)/(10\ \text{min})]^5$) with a final proportion of 100% B. 100% B was maintained until minute 14.5 and then the column was equilibrated in mobile phase A. The ionization by electrospray was carried out in positive mode with a capillary voltage of 3200 V, a source temperature of 110 °C, a desolvation temperature of 500 °C, and a desolvation gas flow of 1000 L h^{-1}.

Surface morphology of the oligoproline-CNF materials. The surface morphology of the oligoproline-CNF materials was examined by scanning electron microscopy (SEM), while SEM with energy dispersive spectroscopy (EDS) was used to observe the surface distribution of the peptide on the CNF material. The samples were prepared by placing a drop of the aqueous suspension on a glass slide and allowing it to dry at room temperature overnight. Afterwards, the samples were mounted on carbon stubs and coated with a conductive thin layer of gold and palladium using a sputter coater Polaron SC7640 sputter coater (Thermo VG Scientific). Samples were imaged using a Zeiss LEO 1550 SEM with a SE2 detector and an energy dispersive detector EDS (Carl Zeiss Microscopy, Oberkochen Germany).

Preparation of double crosslinked CNF hydrogels (Ca^{2+}–oligoproline–CNF). Calcium ions were added to selected oligoproline–CNF materials (Table 1, entries 4 and 6) to obtain a double crosslinked hydrogel, where Ca^{2+} ions are expected to aid in the healing process,[37] and the presence of oligoproline is anticipated to endow CNFs with ROS scavenger properties. Oligoproline–CNF suspensions ($AcKP_5NH_2$–CNF and $AcKP_{10}NH_2$–CNF) at 2 wt% were spread on custom made moulds. Thereafter, the moulds were immersed in 0.1 M $Ca(NO_3)_2$ solution and left at room temperature overnight.[38] Self-standing hydrogels were removed from the moulds and used for further swelling studies (12 mm diameter, 1.5 mm height), rheology studies (size 19 mm diameter, 1.5 mm hight) and cell studies (size 6 mm diameter, 1.5 mm height).

Swelling capacity and degradation of Ca^{2+}–oligoproline–CNF hydrogels. Hydrogels (12 mm in diameter) were weighted after the overnight crosslinking and thereafter placed in PBS to evaluate their swelling capacity. In parallel, the hydrogels were placed in an oxidative environment (H_2O_2 and $CuSO_4$ in PBS, 10 equivalents and 0.05 equivalents respect to the peptide content, respectively) to monitor changes in the hydrogel mass as a consequence of the oxidative degradation of oligoproline. For both experimental conditions, hydrogels were incubated at

Table 1 Screening of experimental conditions for the covalent incorporation of the ROS-sensitive peptide oligoproline to c-CNF through different approaches

Entry	Peptide (equivalents)[a]	Reaction pH	μmol peptide per g CNF[b]	Reaction efficiency (Yield %)[c]	Degree of crosslinking (%)[d]
1	KP_5K (0.1)[e]	5	31 ± 3	17	—
2	KP_5K (0.1)[e]	5.5–6.0, 7.5–8.0	87 ± 8	48	—
3	KP_5K (0.5)[e]	5.5–6.0, 7.5–8.0	110 ± 10	12	—
4	Ac-KP_5K-NH_2 (0.1)	5.5–6.0, 7.5–8.0	102 ± 10	56	80 ± 5
5	Ac-KP_5K-NH_2 (0.5)	5.5–6.0, 7.5–8.0	139 ± 10	15	52 ± 6
6	Ac-$KP_{10}K$-NH_2 (0.1)	5.5–6.0, 7.5–8.0	105 ± 5	58	54 ± 15
7	Ac-$KP_{10}K$-NH_2 (0.5)	5.5–6.0, 7.5–8.0	131 ± 4	15	35 ± 9
8	KP_5K (0.1)[f]	4.5	45 ± 5	34	—
9	KP_5K (0.5)[f]	4.5	137 ± 10	21	—
10	Ac-KP_5K-NH_2 (0.5)[f]	4.5	83 ± 4	13	55 ± 11
11	Ac-KP_5K-NH_2 (0.1)[g]	5.0	68 ± 0.4	38	41 ± 13
12	Ac-KP_5K-NH_2 (0.1)[gh]	5.0	125 ± 8	69	52 ± 11

[a] In comparison with available COOH in c-CNF. [b] By elemental analysis, average of at least three reactions. [c] mmol peptide incorporated/mmol peptide added × 100. [d] crosslinked peptide/total incorporated peptide × 100. [e] Unreacted EDC, NHS and by-products were washed out before peptide addition. [f] Reductive amination of previously oxidised c-CNF, in comparison with available COH in c-CNF. [g] Physical adsorption followed by covalent immobilization. [h] High concentration c-CNF (c-CNF concentration in the reaction mixture = 2 wt%).

37 °C for 4 days, the hydrogel weight was monitored daily using a high precision scale (XA205DU Mettler Toledo, Belgium) and solutions were refreshed every day. The remaining weight was expressed as the percentage of the initial weight.

Viscoelastic properties of Ca^{2+}–oligoproline–CNF hydrogels exposed to oxidative conditions. The rheological characterization of the double crosslinked oligoproline-CNF hydrogels was performed using a Discovery HR-3 Hybrid (TA instrument, New Castle, United States) equipped with a parallel plate geometry (20 mm diameter). Hydrogels were loaded onto the Peltier plate; the geometry was lowered and the gap was controlled by applying a constant axial force of 0.2 ± 0.1 N to ensure constant contact between the geometry and the hydrogel. Samples were allowed to equilibrate for 60 s before the start of the procedure and all experiments were performed at 25 °C in the oscillatory mode. First, an amplitude sweep from 0.01% to 10% strain at 1 Hz oscillation frequency was performed to determine the linear viscoelastic region (LVR) of the materials, where stress and strain are proportional (Fig. S2, ESI†). A strain of 0.25% was selected to evaluate the frequency dependence of the dynamic moduli G' and G''.[39] Thereafter, frequency sweep from 0.01 to 10 Hz at 0.25% strain was performed and the frequency-dependence of the storage (G') and loss (G'') modulus was evaluated as the indicator of the viscoelastic response of the double crosslinked hydrogels.

The response of the hydrogels (Ca^{2+}–AcKP_5NH_2–CNF and Ca^{2+}–Ac$KP_{10}NH_2$–CNF) to an oxidative environment was investigated by evaluating the change in their viscoelastic properties. Hydrogels were incubated with 5 mL of 6 mM H_2O_2 and 30 μM $CuSO_4$ in PBS for 4 days at 37 °C, refreshing the solution daily. As a control, hydrogels were incubated in PBS at 37 °C for 4 days and the solution was also renewed daily. Rheology measurements were done on day 0 and day 4 with different samples, and conditions were run in duplicate.

Cell protective effect of Ca^{2+}–oligoproline–CNF hydrogels under oxidative conditions.

Cell culture. Adult human dermal fibroblasts (hDFs, European Collection of Authenticated Cell Cultures, EACC) were cultured in DMEM-F12 medium supplemented with 10% v/v FBS, 100 U mL^{-1} penicillin, and 100 μg mL^{-1} streptomycin. Cells were cultured at 37 °C and 5% CO_2 in a humidified atmosphere and passaged at 80% confluency.

Cell protective effect study. The capacity of the Ca^{2+}–oligoproline–CNF hydrogels to protect cells exposed to an oxidative environment was investigated by simultaneously exposing monolayers of hDF cells to the hydrogels and high levels of H_2O_2. hDF cells (passage numbers 10 to 17) were seeded in 96-well plates at a density of 4800 cells per well and cultured for 24 hours. Ca^{2+}–AcKP_5NH_2–CNF and Ca^{2+}–Ac$KP_{10}NH_2$–CNF hydrogels, previously rinsed with sterile MiliQ water and then soaked in cell culture medium, were placed carefully on top of the cell monolayer, followed by the addition of 200 μL of 350 μM H_2O_2 in cell culture medium to each well and cells were culture for additional 72 hours. To ensure a constant oxidative environment, the H_2O_2 solution was refreshed daily. Non-exposed cells were considered the negative control and cells exposed to H_2O_2 alone served as positive control. Cells were also exposed to the hydrogels alone to evaluate the effect of the hydrogels on cell proliferation and viability. The cell culture medium of the groups not exposed to H_2O_2 was also replaced daily as to mimic the procedure with the group exposed to H_2O_2. After 72 hours, cell culture medium was aspirated and 150 μL of live/dead staining solution (0.2% v/v calcein-AM and 0.1% v/v propidium iodide in PBS) was added to each well and incubated for 15 min at 37 °C, 5% CO_2 and humidified atmosphere. The staining solution was removed and 200 μL pre-warmed cell culture medium was added to each well. Cells were imaged using a confocal microscope (Leica SP8, Wetzlar, Germany) to evaluate cell viability and morphology. At least three independent experiments in triplicate were performed.

Results and discussion

Developing ROS-sensitive CNF materials

In this work, we describe the covalent incorporation of oligoproline peptides onto c-CNF by well-known chemical approaches. The presence of the ROS-sensitive peptide is expected to endow CNFs with ROS-scavenger properties, a characteristic that could be exploited for the development of CNF-based dressings for the treatment of chronic wounds. Besides, to crosslink the nanofibres with the ROS-sensitive peptide opens up for the possibility of developing responsive hydrogels, which could be useful in

tissue engineering and drug delivery applications. Incorporation of aminoacids or peptides to nanocellulose (mainly cellulose nanocrystals) have been described in the literature, being EDC/NHS coupling the most used chemical approach.[35,40–42] The coupling of amines with carboxyl groups through EDC/NHS is sensitive to pH[43] and the formed intermediates are unstable when the reaction is carried out using water as the reaction solvent, with the possibility of hydrolysis and consequently reaction failure. A pH between 5 and 6 is considered to be optimal to carry out the activation of carboxylic acids by EDC.[44] On the other hand, a pH of 8.5–9.5 is generally preferred for modifying lysine residues (deprotonated ε-amino groups) but unfortunately the intermediates formed during the reaction are more unstable at the same time that pH is more basic. Thus, the sensitivity of the reaction to pH together with the lack of solubility of c-CNF (heterogeneous conditions), means that an optimization of the reaction conditions needs to be done with the aim of obtaining an efficient covalent immobilization of the peptide and a high degree of crosslinking of the fibres.

As summarized in Table 1, the screening of the reaction was carried out with a series of oligoproline peptides previously described (Fig. 1). Each reaction was performed three times to confirm reproducibility. Two different concentrations of oligoproline peptide were used during the optimization, 10% peptide (0.1 equivalents) and 50% peptide (0.5 equivalents) relative to the number of COOH groups in c-CNF. The aim of using these concentrations is to find a balance between the degree of incorporation of peptide and promoting the crosslinking of the nanofibres by the peptide.

Initial experiments began using the oligoproline peptide KP_5K, which sequence contains five proline units (P_5) between two units of lysine (K). Free primary amines (NH_2) from lysine amino acid are expected to react with carboxylic acids groups on the surface of c-CNF. As anticipated, an increase in the incorporation of peptide was detected by tuning the pH between the carboxylic acid activation and the amine-coupling step (31 ± 3 μmol peptide per g CNF *vs.* 87 ± 8 μmol peptide per g CNF, entry 1 *vs.* entry 2).

Afterwards, studies with Ac-KP_5K-NH_2 were carried out. Having the carboxylic acid protected can minimize side reactions and avoid repulsion effects between the fibres and the peptide due to extra negative charges. Furthermore, protecting the α-amine gives more control over the reaction, *i.e.* only the terminal amine is able to react with the carboxyl groups and also allows to use the ninhydrin assay to evaluate the crosslinking rate.

Subsequently, the peptide Ac-$KP_{10}K$-NH_2 was used in order to study the impact of increasing the units of proline on the chemical modification and on the response of the material to ROS (see material characterization). The reactivity was very similar between 5 prolines peptide (entries 4–5) and 10 prolines peptide (entries 6–7), thus oligoproline with different lengths can be incorporated onto CNFs with similar yields.

The reaction efficiency (Table 1) was probably limited by the bulky effect caused by the size of the peptides, as the amount of covalently incorporated peptide was not efficiently increased when increasing the amount of reacting peptide (entries 2–7). The maximum peptide substitution obtained was 139 ± 10 μmol peptide per g CNF when using 0.5 equivalents of the shorter oligopeptide (Table 1, entry 5); however, the reaction yield was only 15%. A preliminary study demonstrated that an increase in the initial amount of peptide to 2 equivalents relative to the number of COOH groups in c-CNF did not increase the degree of peptide incorporation (results not shown).

As an alternative chemical procedure, ROS-sensitive peptides (KP_5K and Ac-KP_5K-NH_2) were incorporated onto CNFs by reductive amination of previously oxidised c-CNF (entries 8–10). The results showed that increasing the amount of peptide KP_5K from 10% peptide (0.1 equivalents) to 50% (0.5 equivalents) peptide relative to COH of periodate-oxidized c-CNF gave a substantial increase in the amount of peptide incorporated to c-CNF (45 ± 5 μmol peptide per g CNF *vs.* 137 ± 10 μmol peptide per g CNF, entry 8 *vs.* entry 9). Overall, the amount of incorporated peptide with this method was comparable with the results obtained with the EDC/NHS method.

A second aim of the optimization of the reaction conditions was to achieve a high degree of fibre crosslinking with the ROS sensitive peptide, as a way of adding extra functionality to the CNF material. The degree of crosslinking was evaluated by the ninhydrin assay in the materials $AcKP_5KNH_2$–CNF and $AcKP_{10}KNH_2$–CNF obtained by the different chemical approaches and results showed that the highest degree of crosslinking was found when the EDC/NHS coupling was carried out, with a degree of crosslinking of 80% for $AcKP_5NH_2$–CNF (entry 4, Table 1). An increase in the incorporation of peptide (entry 5, Table 1) or the peptide length (entries 6 and 7, Table 1) had a negative impact on the degree of crosslinking. An increase in the repulsion between the fibres due to the covalently bound peptide could explain such a decrease in the degree of crosslinking, a repulsion that may prevent the one end-attached peptide to encounter free carboxyl groups in neighbour fibres and crosslink the fibres. This negative effect of increasing the linker grafting on the degree of crosslinking has been observed by other authors, when crosslinking CNFs with polyethylene glycol[44] and also when working with other materials and chemical reactions.[45]

As an attempt to overcome the above limitation, $AcKP_5KNH_2$–CNF materials were developed by using two other approaches. In the first approach, electrostatic interactions were favoured (physical adsorption followed by covalent immobilization) between the peptide and c-CNF before the covalent bond was formed (68 ± 0.4 μmol peptide per g CNF, entry 11). In a second approach, and with the aim of having the CNF fibres closer to each other and thus favour the crosslinking, the modification was performed following the same procedure but with c-CNF at a high concentration (2 wt%) in the reaction mixture (125 ± 8 μmol peptide per g CNF, entry 12). Neither of these chemical approaches improved the crosslinking rate obtained by the EDC/NHS coupling (80%, entry 4 *vs.* 41% and 52%, entries 11 and 12 respectively).

In summary, the different chemical approaches gave comparable results in terms of the degree of substitution and reaction efficiency, independently of the length of the oligoproline peptide used. Thus, the EDC/NHS coupling was chosen as the preferable method due to the reaction feasibility and higher degree of

crosslinking obtained with this method compared with the other approaches.

Material characterization. The material KP_5K–CNF (110 μmol peptide per g CNF, entry 3, Table 1) was selected to investigate the chemical structure and its susceptibility to ROS-mediated degradation. The functionalization of c-CNF with KP_5K was detected by CP/MAS ^{13}C-NMR spectroscopy. The CP/MAS ^{13}C-NMR spectrum of KP_5K-CNF is displayed in Fig. 3 together with the spectrum of c-CNF and free peptide as references. The signals between 23 and 53 ppm in KP_5K–CNF are attributed to pyrrole and sidechain carbons in the peptide. The carbon close to the terminal NH_2 is upfield shifted (from 40.59 ppm to 35.89 ppm) in KP_5K–CNF if compared to the free peptide, which agrees with the formation of a covalent amide bond between the ε-amine of the peptide and the carboxylic acids of c-CNF. CP/MAS ^{13}C-NMR analysis was further used to compare the degree of crosslinking and concentration of the peptide in the different $AcKP_5NH_2$–CNF materials, showing that the information obtained from the spectra correlated with the results found by elemental analysis and the ninhydrin test (Fig. S3, ESI†).

Next, the susceptibility of KP_5K–CNF to an oxidative environment was studied. In such environment, oligoproline is expected to undergo radical-mediated cleavage.[12] ROS-mediated oxidation takes place by a mechanism involving the oxidation of the proline residues to 2-pyrrolidone derivative by hydroxyl radicals generated from H_2O_2 and $CuSO_4$ (Scheme S1, ESI†).[12,17] The tertiary amide bonds in proline are more susceptible to oxidation than secondary amide bonds, making proline more reactive to ROS than the other amino acids known to be susceptible to ROS-mediated oxidation (*i.e.* histidine, arginine and lysine).[13]

KP_5K–CNF and KP_5K were incubated under oxidative conditions using H_2O_2 and the degradation of oligoproline was investigated by LC-MS. New compounds due to the peptide backbone cleavage, with different retention time and lower molecular weight (*e.g.* *m*/*z* 195.130, 226.155 and 355.198) than the parent oligopeptide were detected by LC-MS when the free KP_5K was exposed to the oxidative environment (Fig. 4b), while the oligopeptide was stable in the absence of oxidative conditions (Fig. 4a). KP_5K-CNF exposed to the oxidative environment showed an oxidation profile comparable to the profile of the free peptide (Fig. 4c). c-CNF was also tested in oxidative conditions and PBS, showing complete stability in both conditions, during 4 days of stirring at 37 °C, without extra compounds detected by LC-MS (Fig. 4d and e). Overall, the immobilized oligoproline was susceptible to the oxidation-induced cleavage and the response of the oligoproline–CNF material to an oxidative environment can be attributed primarily to the oligopeptide and not to any side reaction with the CNF matrix. Furthermore, an increase in the concentration of the oxidation by-products could be observed over time (Fig. S4, ESI†).

Two oligoproline–CNF materials were selected for further characterization, $AcKP_5NH_2$–CNF and $AcKP_{10}NH_2$–CNF (Table 1, entries 4 and 6), *i.e.* materials functionalized with 5 and 10 units of proline which presented both relatively high reaction efficiency and high degree of crosslinking. Fibre morphology of these functionalized CNF materials was evaluated with SEM,

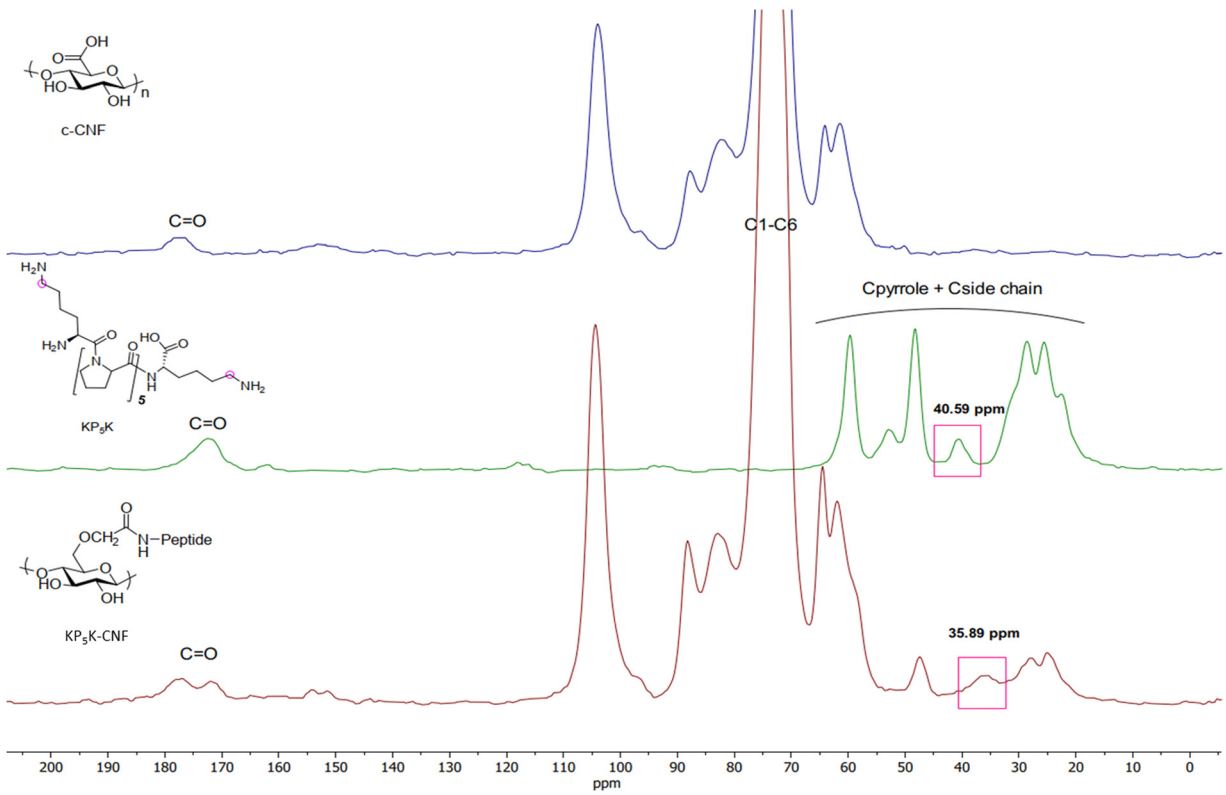

Fig. 3 Solid-state nuclear magnetic resonance (CP/MAS ^{13}C-NMR) spectra of KP_5K-CNF and the references c-CNF and KP_5K oligopeptide.

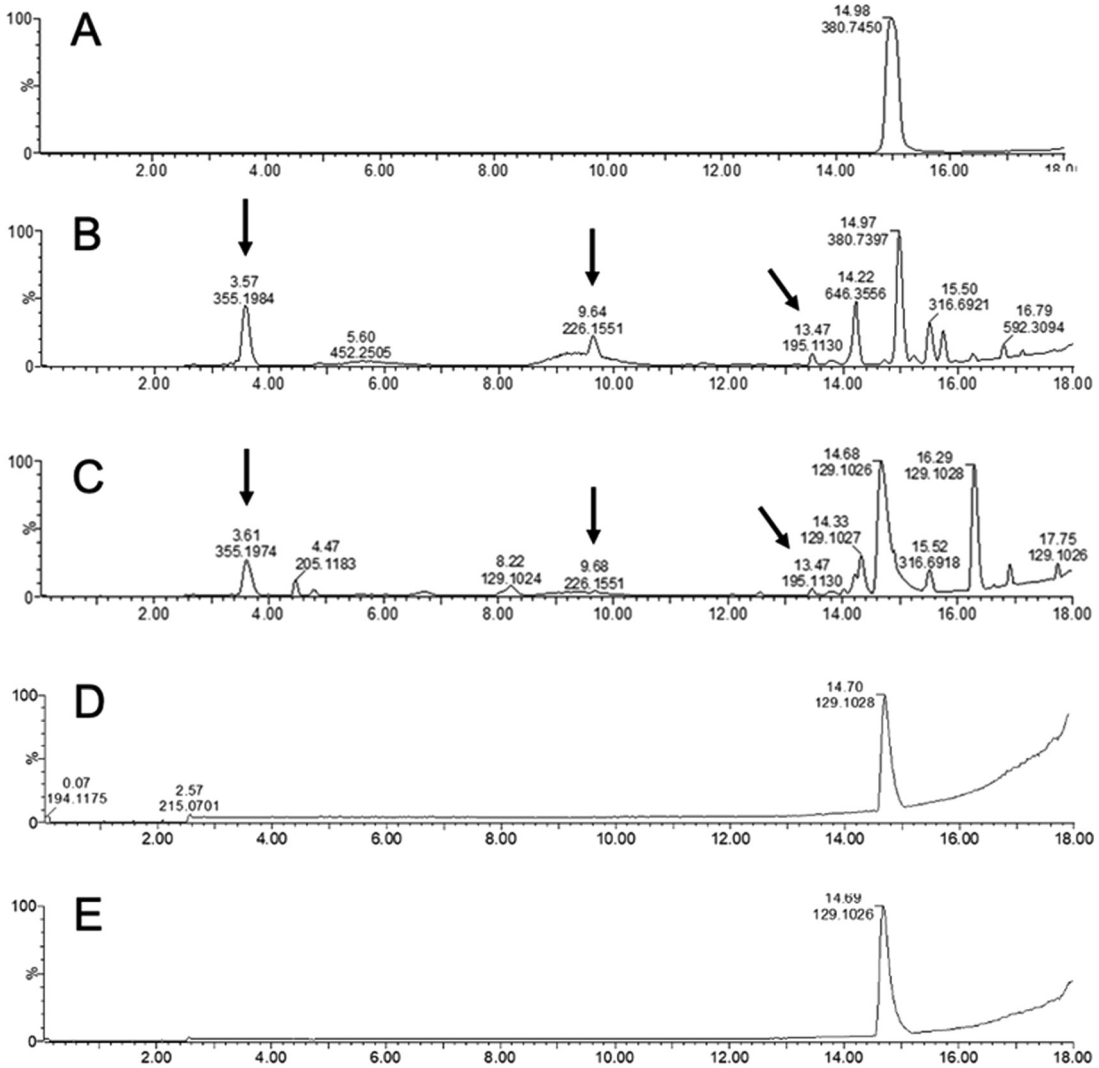

Fig. 4 Liquid chromatography-mass spectrometry profile (BPI, base peak ion) of KP_5K incubated at 37 °C for 4 days in PBS (4a), KP_5K incubated at 37 °C for 4 days in PBS containing H_2O_2 and Cu(II) (4b), KP_5K-CNF incubated at 37 °C for 4 days in PBS containing H_2O_2 and Cu(II) (4c), c-CNF incubated at 37 °C for 4 days in PBS (4d) and c-CNF incubated at 37 °C for 4 days in PBS containing H_2O_2 and Cu(II) (4e). New by-products with lower molecular weight than the original peptide as a consequence of oxidative cleavage (*m/z* 195.130, 226.155 and 355.198) were detected in the spectrum of both KP_5K and KP_5K-CNF.

with the images showing that the covalent incorporation of the peptides did not have a significant effect on the morphology of the fibres compared with the starting material c-CNF, with all materials showing randomly oriented fibrils (Fig. 5). The analysis of the materials by SEM-EDS revealed a homogeneous distribution of nitrogen on the material surface for both oligoproline materials, thus indicating that the covalently bound peptides were uniformly distributed along the fibres (Fig. 6).

The cytotoxicity of the selected oligoproline-CNF materials was investigated *in vitro* with hDFs. Results showed that none of the materials significantly affected the cell metabolic activity of the cells when tested at concentrations ranging from 0.1 to 1 mg ml^{-1} (Fig. S5, ESI†). Hence, the introduction of the oligoproline peptides, as expected, did not affect the previously shown non-toxic profile of the c-CNF material,[46] and these results also confirmed the successful washing steps for the removal of reactants that potentially could affect the cells.

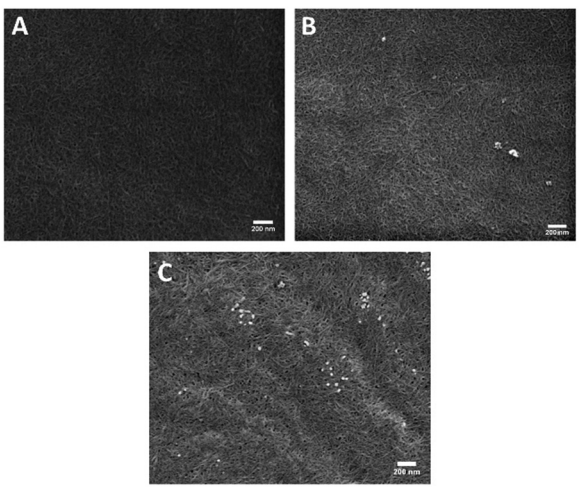

Fig. 5 Representative scanning electron microscopy images of (a) c-CNF, (b) $AcKP_5NH_2$-CNF and (c) $AcKP_{10}NH_2$-CNF. Scale bars represent 200 nm.

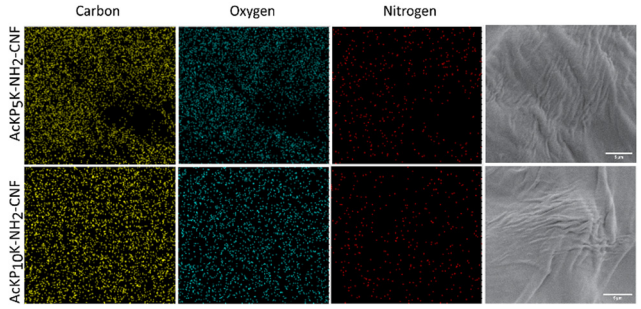

Fig. 6 Representative images of the scanning of carbon, oxygen and nitrogen by SEM-EDS of $AcKP_5NH_2$-CNF (upper panels) and $AcKP_{10}NH_2$-CNF (lower panels) and the corresponding SEM images (scale bars represent 5 μm).

Regarding the viscoelastic characteristics of the oligoproline-CNF materials, it should be mentioned that the high degree of crosslinking of the materials (80% in the case of $AcKP_5NH_2$–CNF and 54% for $AcKP_{10}NH_2$–CNF) was not reflected in significant changes in the viscoelastic properties of the materials compared with the starting c-CNF (results not shown). Even though 80% of the attached peptides were crosslinking the cellulose nanofibres, the level of peptide substitution (102 ± 10 μmol g^{-1} CNF) and therefore the maximum number of possible crosslinks was not enough to significantly increase the storage modulus of the hydrogels compared to the c-CNF gel suspension.

Double-crosslinked CNF hydrogels: towards bioactive hydrogels for chronic wound care. Double-crosslinked CNF hydrogels (Fig. 7(III)) were prepared to combine the covalent crosslinking with the ROS scavenger peptide and the ion crosslinking with Ca^{2+}. Calcium-crosslinked CNF hydrogels have previously shown promising results accelerating the healing of acute wounds,[26] while the crosslinking with oligoproline is expected to endow the hydrogel with ROS-scavenger properties, a property that can be beneficial when developing a wound dressing for the treatment of chronic wounds.

The swelling capacity of the as-prepared hydrogels was evaluated. Results showed that the as-prepared hydrogels did not significantly swell when further incubated in PBS over 4 days, since no significant changes in the hydrogel weight were observed during the incubation period (Fig. S6, ESI†).

Particularly interesting is to evaluate the effect of the radical cleavage of the oligoproline crosslinker on the rheological properties of the hydrogels. Thus, the viscoelastic properties of the double-crosslinked hydrogels were studied in the absence and presence of high levels of ROS. Ca^{2+}–$AcKP_5NH_2$–CNF hydrogels incubated in H_2O_2 for 4 days showed a decrease in G', however such behavior was comparable to the sample incubated in PBS (Fig. 7(I)). This implies that the main contribution to the reduction in storage modulus came from the ion exchange of the Ca^{2+} crosslinker, rather than the oxidative cleavage of the oligoproline peptide. Nevertheless, in the case of Ca^{2+}–$AcKP_{10}NH_2$–CNF samples, hydrogels incubated in H_2O_2 for 4 days showed a higher decrease in storage modulus than the samples in PBS (Fig. 7(I)). Thus, indicating that in this case, the ROS-mediated degradation of the 10-unit oligoproline had a significant contribution to the observed changes in the viscoelastic properties of the hydrogel. It should be noted that both

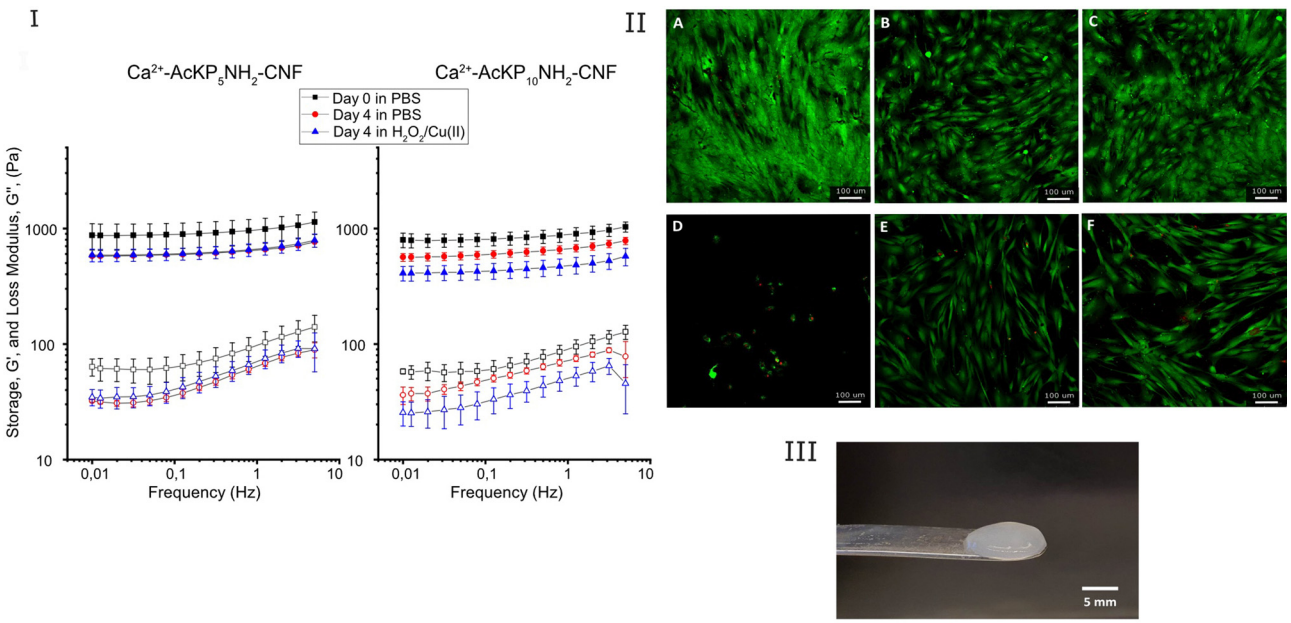

Fig. 7 Characterization of double crosslinked hydrogels. (I) Viscoelastic properties of double crosslinked Ca^{2+}-oligoproline-CNF hydrogels exposed to an oxidative environment for 4 days compared to gels exposed to phosphate buffered saline (PBS). Filled symbols correspond to storage modulus G′ and empty symbols to loss modulus G″. Data correspond to average values with the standard deviation. (II) Live/dead staining of hDFs exposed to the double crosslinked Ca^{2+}-oligoproline-CNF hydrogels under high levels of ROS. Panels A, B and C correspond to cells in cell culture medium; D, E and F correspond to cells in an oxidative environment; A, D without hydrogel; B, E with Ca^{2+}-$AcKP_5NH_2$-CNF hydrogel and C, F with Ca^{2+}-$AcKP_{10}NH_2$-CNF hydrogel. Scale bar corresponds to 100 μm. (III) Representative image of the double crosslinked Ca^{2+}-oligoproline-CNF hydrogels.

oligoproline–CNF materials have a similar degree of peptide substitution and $AcKP_5NH_2$–CNF has an even higher degree of crosslinking than $AcKP_{10}NH_2$–CNF, so the difference in ROS response may be attributed to the different length of the oligoproline. The ROS-mediated cleavage of oligoproline seems to be more efficient when the number of proline units increases. Kawasaki *et al.* showed similar results when comparing the sensitivity to ROS of oligoprolines with different lengths[17] while Yu *et al.* established that the degradation rate of PEG–oligoproline–PEG crosslinkers was proportional to the length of the oligoproline within the crosslinkers.[22]

The ROS-mediated cleavage of the crosslinkers was not reflected in significant changes in the weight of the hydrogels (Fig. S6, ESI†). This could be explained by the fact that the cleavage of the oligoproline linker results in a relaxation of the hydrogel matrix and as a consequence, an influx of water to the hydrogel network occurs,[47] compensating for the loss of oligoproline mass.

Another valuable evaluation of the double crosslinked hydrogels, having in mind the potential use in chronic wound care, is the ability of the hydrogels to protect cells from an oxidative environment. The cell protective effect of the Ca^{2+}–$AcKP_5NH_2$–CNF and Ca^{2+}–$AcKP_{10}NH_2$–CNF hydrogels against high levels of ROS was evaluated *in vitro* with hDFs. The hydrogels were placed on top of cell monolayers while the cells were exposed to high levels of H_2O_2 for 72 h. First, controls in the absence of H_2O_2 showed that the cells were able to proliferate in the presence of the hydrogels. Cells under the hydrogels showed slightly less confluency than the unexposed cells, but no significant cell membrane damage was observed (red staining) and cells displayed the characteristic morphology of fibroblasts (Fig. 7(II), panels A, B and C). The presence of the hydrogels when cells were exposed to the oxidative environment resulted in a significant increase in cell survival compared to cells exposed to H_2O_2 in the absence of the hydrogels (Fig. 7(II) panels D, E, F). This suggests that the oligoproline-CNF hydrogels were able to protect the cells from the oxidative environment, an effect that most probably can be attributed to the oligoproline capability of consuming ROS.[13] Moreover, the byproducts from the oligoproline cleavage under oxidative conditions did not induce signs of cytotoxicity in hDFs. The observed cell protecting effect of the Ca^{2+}–oligoproline–CNF materials opens up further investigation on the use of the hydrogels for cell therapy in chronic wound care.

Conclusions

The present work showed the successful covalent incorporation of oligoproline onto CNFs *via* carbodiimide chemistry, obtaining a CNF-based material able to respond to high levels of ROS. Double crosslinked Ca^{2+}–oligoproline–CNF hydrogels protected cells from oxidative conditions, while ROS-mediated changes in the viscoelastic properties of the hydrogels depended on the length of the immobilized oligoproline. These results push forward the investigation of ROS-sensitive CNF-based materials as advanced solutions for the treatment of chronic wounds and other clinical conditions associated with high levels of ROS.

Conflicts of interest

There are no conflicts to declare.

Acknowledgements

The authors would like to thank Lulu Wu, Division of Nanotechnology and Functional Materials, Uppsala University for her valuable assistance with the scanning electron microscope. This research was funded by the Swedish Research Council (grant number 2018-04613) and Olle Engkvists Stiftelse (grant number 191-419).

Notes and references

1 M. Pääkkö, M. Ankerfors, H. Kosonen, A. Nykänen, S. Ahola, M. Österberg, J. Ruokolainen, J. Laine, P. T. Larsson, O. Ikkala and T. Lindström, *Biomacromolecules*, 2007, **8**, 1934–1941.
2 D. Klemm, D. Schumann, F. Kramer, N. Heßler, M. Hornung, H.-P. Schmauder and S. Marsch, *Polysaccharides*, 2006, **205**, 49–96.
3 N. Jamaluddin, T. Kanno, T.-A. Asoh and H. Uyama, *Mater. Today Commun.*, 2019, **21**, 100587.
4 R. Curvello, V. S. Raghuwanshi and G. Garnier, *Adv. Colloid Interface Sci.*, 2019, **267**, 47–61.
5 K. Heise, G. Delepierre, A. W. T. King, M. A. Kostiainen, J. Zoppe, C. Weder and E. Kontturi, *Angew. Chem., Int. Ed.*, 2021, **60**, 66–87.
6 K. J. de France, T. Hoare and E. D. Cranston, *Chem. Mater.*, 2017, **29**, 4609–4631.
7 H. N. Abdelhamid and A. P. Mathew, *Int. J. Mol. Sci.*, 2022, **23**, 5405.
8 N. Fatema, R. M. Ceballos and C. Fan, *Front. Bioeng. Biotechnol.*, 2022, **10**, 1.
9 K. Heise, E. Kontturi, Y. Allahverdiyeva, T. Tammelin, M. B. Linder, Nonappa and O. Ikkala, *Adv. Mater.*, 2021, **33**, 2004349.
10 T. V. Patil, D. K. Patel, S. D. Dutta, K. Ganguly, T. S. Santra and K.-T. Lim, *Bioact. Mater.*, 2022, **9**, 566–589.
11 R. Tarrahi, A. Khataee, A. Karimi and Y. Yoon, *Chemosphere*, 2022, **288**, 132529.
12 Q. Xu, C. He, C. Xiao and X. Chen, *Macromol. Biosci.*, 2016, **16**, 635–646.
13 H. Ye, Y. Zhou, X. Liu, Y. Chen, S. Duan, R. Zhu, Y. Liu and L. Yin, *Biomacromolecules*, 2019, **20**, 2441–2463.
14 G. Saravanakumar, J. Kim and W. J. Kim, *Adv. Sci.*, 2017, **4**, 1600124.
15 C. Tapeinos and A. Pandit, *Adv. Mater.*, 2016, **28**, 5553–5585.
16 E. R. Stadtman and R. L. Levine, *Amino Acids*, 2003, **25**, 207–218.
17 R. Kawasaki, K. Tsuchiya, Y. Kodama and K. Numata, *Biomacromolecules*, 2020, **21**, 4116–4122.
18 M. Mardirossian, R. Sola, B. Beckert, D. W. P. Collis, A. di Stasi, F. Armas, K. Hilpert, D. N. Wilson and M. Scocchi, *ChemMedChem*, 2019, **14**, 2025–2033.

19 M. G. Gagnon, R. N. Roy, I. B. Lomakin, T. Florin, A. S. Mankin and T. A. Steitz, *Nucleic Acids Res.*, 2016, **44**, 2439–2450.
20 N. G. Welch, W. Li, M. A. Hossain, F. Separovic, N. M. O'Brien-Simpson and J. D. Wade, *Front. Chem.*, 2020, **8**, 607769.
21 S. H. Lee, T. C. Boire, J. B. Lee, M. K. Gupta, A. L. Zachman, R. Rath and H. J. Sung, *J. Mater. Chem. B*, 2014, **2**, 7109–7113.
22 S. S. Yu, R. L. Koblin, A. L. Zachman, D. S. Perrien, L. H. Hofmeister, T. D. Giorgio and H.-J. Sung, *Biomacromolecules*, 2011, **12**, 4357–4366.
23 M. K. Gupta, S. H. Lee, S. W. Crowder, X. Wang, L. H. Hofmeister, C. E. Nelson, L. M. Bellan, C. L. Duvall and H. J. Sung, *J. Mater. Chem. B*, 2015, **3**, 7271–7280.
24 R. F. Diegelmann, *Front. Biosci.*, 2004, **9**, 283.
25 T. N. Demidova-Rice, M. R. Hamblin and I. M. Herman, *Adv. Skin Wound Care*, 2012, **25**, 304–314.
26 E. Öhnstedt, H. Lofton Tomenius, E. Vågesjö and M. Phillipson, *Expert Opin. Drug Discovery*, 2019, **14**, 485–497.
27 S. A. Eming, P. Martin and M. Tomic-Canic, *Sci. Transl. Med.*, 2014, **6**, 265.
28 R. G. Frykberg and J. Banks, *Adv. Wound Care*, 2015, **4**, 560–582.
29 A. Basu, G. Celma, M. Strømme and N. Ferraz, *ACS Appl. Bio Mater.*, 2018, **1**, 1853–1863.
30 A. Basu, J. Hong and N. Ferraz, *Macromol. Biosci.*, 2017, **17**, 1700236.
31 A. Basu, J. Lindh, E. Ålander, M. Strømme and N. Ferraz, *Carbohydr. Polym.*, 2017, **174**, 299–308.
32 K. Hua, D. O. Carlsson, E. Ålander, T. Lindström, M. Strømme, A. Mihranyan and N. Ferraz, *RSC Adv.*, 2014, **4**, 2892–2903.
33 H. Zhao and N. D. Heindel, *Pharm. Res.*, 1991, **8**(3), 400–402.
34 H. Wang, R. Liu, Y. Liu, Y. Meng, Y. Liu, H. Zhai and D. Di, *Langmuir*, 2019, **35**, 4471–4480.
35 J. V. Edwards, K. R. Fontenot, D. Haldane, N. T. Prevost, B. D. Condon and C. Grimm, *Cellulose*, 2016, **23**, 1283–1295.
36 P. Eiselt, K. Y. Lee and D. J. Mooney, *Macromolecules*, 1999, **32**, 5561–5566.
37 T. Subramaniam, M. B. Fauzi, Y. Lokanathan and J. X. Law, *Int. J. Mol. Sci.*, 2021, **22**, 6486.
38 H. Dong, J. F. Snyder, K. S. Williams and J. W. Andzelm, *Biomacromolecules*, 2013, **14**, 3338–3345.
39 J. M. Zuidema, C. J. Rivet, R. J. Gilbert and F. A. Morrison, *J. Biomed. Mater. Res., Part B*, 2014, **102**, 1063–1073.
40 S. Barazzouk and C. Daneault, *Nanomaterials*, 2012, **2**, 187–205.
41 V. Gabrielli, E. Missale, M. Cattelan, M. F. Pantano and M. Frasconi, *Mater. Today Chem.*, 2022, **24**, 100886.
42 R. T. Mackin, K. R. Fontenot, J. V. Edwards, N. T. Prevost, C. Grimm, B. D. Condon, F. Liebner, J. H. Jordan, M. W. Easson and A. D. French, *Cellulose*, 2022, **29**, 1293–1305.
43 R. K. Johnson, A. Zink-Sharp and W. G. Glasser, *Cellulose*, 2011, **18**, 1599–1609.
44 T. Kaldéus, M. Nordenström, A. Carlmark, L. Wågberg and E. Malmström, *Carbohydr. Polym.*, 2018, **181**, 871–878.
45 J. Pupkaite, J. Rosenquist, J. Hilborn and A. Samanta, *Biomacromolecules*, 2019, **20**, 3475–3484.
46 V. R. Lopes, C. Sanchez-Martinez, M. Strømme and N. Ferraz, *Part. Fibre Toxicol.*, 2017, **14**, 1.
47 Polymeric Hydrogels as Smart Biomaterials, *Springer Series on Polymer and Composite Materials Series*, ed. S. Kalia, 2016.